Rectified Flows over a Finite Length Shelf Break: a Bank and a Canyon Case

J. Verron, D. Renouard

Laboratoire des Ecoulements Géophysiques et Industriels, URA 1509 CNRS, BP 53X, 38041 Grenoble Cedex, France

D. L. Boyer

Environment Fluid Dynamics Program and Department of Mechanical and Aerospace Engineering, Arizona State University, Tempe, AZ 85287-1903

Abstract.
Rectified processes over a submerged elongated bank and over a canyon in an otherwise long shelf break were investigated by means of numerical and laboratory experiments for the bank and by means of numerical experiments only for the canyon.
The physical experiments were conducted in the Grenoble 13 m diameter rotating tank. The background oscillating motion was obtained by periodically varying the platform angular velocity. Fluid motions were visualized and quantified by direct velocity mesurements and particle tracking. The numerical model employed was a tridimensional model developed by *Haidvogel et al.* [1991]. It consists of the traditional primitive equations; i.e., the Navier-Stokes equations for a rotating fluid with the addition of the hydrostatic, Boussinesq and incompressibility approximations.
In the bank case, both the laboratory and numerical experiments show that in the range of dimensionless parameters considered, two distinct flow regimes, based on general properties of the rectified flow patterns observed, can be defined. It is further shown that the flow regime designation depends principally on the magnitude of the temporal Rossby number, Ro_t, defined as the ratio of the flow oscillation to the background rotation frequency. Good qualitative and quantitative agreement is found between the laboratory experiments and the numerical model for such observables as the spatial distribution of rectified flow patterns.
In the canyon case, although the geometry is quite different, strong similarities are observed especially the existence of flow regimes having a strong analogy with the ones identified in the previous case. The temporal Rossby number, Ro_t, is also an essential controlling parameter although the standard Rossby number, Ro, interplays significantly. The most important result however, in this case, is the capability for the canyon to be a downstream source of mean rectified current at distances which are large with regard to the horizontal scale of the canyon .

Introduction

The nonlinear generation of a mean flow by oscillatory or other unsteady currents or turbulence (i.e. rectification), is for the most part studied in relation to the ubiquitous presence of tides. Such rectification processes have been observed in numerous places, for instance along the Georges Bank [*Butman et al.*, 1982; *Tee*, 1985] and along the La Chapelle Bank [*Garreau and Mazé*, 1991]. There are also observations of rectified flows around Bermuda [*Stommel*, 1954], Fieberling Guyot in the North Pacific [*Genin et al.*, 1989; *Eriksen*, 1991], in the Bay of Biscay [*Pingree and Le Cann*, 1990], in the Straits of Dover [*Brylinski and Lagadeuc*, 1990] and the North Sea [*Maas and Van Haren*, 1987]. Rectification may not be only driven by tides but by a complete spectrum of motions as discussed by *Holloway* [1987]. This may include for example, long and short periods of wind forcing [*Haidvogel and Brink*, 1986].

Whatever the direction of the unsteady forcing flow is, the local mean rectified flow is in a direction such that the shallow water is on the right, facing downstream (in the Northern Hemisphere). In the case of a simple slope, the topographically equivalent β-effect will therefore induce a rectified "westward-equivalent" current. The amplitude of this rectified flow can be a significant fraction of the amplitude of the forcing flow. Consequently, rectification can contribute significantly to mean current systems in the vicinity of the shelf break and, by extension, to the structure of the coastal current system itself.

In the context of tides, *Robinson* [1981] described three possible generation mechanisms for a rectified flow: (i) the change in relative vorticity necessary for the conservation of potential vorticity, (ii) the generation of vorticity when there is lateral shear in a flow, even when the depth is uniform, and (iii) the generation of vorticity due to the shear in the depth distributed friction force when there is a depth variation

in a direction normal to the local velocity. The second mechanism appears only if one adopts a quadratic representation of the bottom friction. Note that depth variation alone, may be sufficient to support rectification. *Zimmerman* [1978] derived the applicable vorticity equation depending on the presence of depth variations and Coriolis and viscous effects. It is seen that rectification requires a phase shift between the vorticity field and the background tidal current.

Among the theoretical studies employing these mechanisms for depth independent models are those of *Huthnance* [1973, 1981], *Zimmerman* [1978, 1980], *Tang and Tee* [1987], *Loder* [1980] and *Loder and Wright* [1985]. *Maas and Zimmerman* [1989a, 1989b] have developed a numerical model for oscillatory, stratified flow normal to infinitesimal shelf breaks. Their resulting along- and cross-isobath residual and tidal circulations and isopycnal elevations have a well-defined localized structure in the cross-isobath vertical plane. More recently, *Chen* [1992] considered numerically the tidal rectification of a stratified ocean in the vicinity of two-dimensional model topography, including a model for Georges Bank, and suggests that stratification plays a significant role in the spatial structure of the rectified currents. *Garreau and Mazé* [1991] developed an interpretative model for their observations near La Chapelle bank in which they indicated that the nonlinear dynamics of an inviscid ocean can act as a flow rectification mechanism.

Motivated by field observations in the vicinity of Fieberling Guyot, *Boyer et al.* [1991] studied the oscillatory motion of a homogeneous, rotating fluid in the vicinity of an isolated topographic feature, both in the laboratory and numerically. The experiments clearly showed that a mean anticyclonic vortex is formed above the topographic feature, and that the spatial and temporal Rossby numbers of the background flow are key parameters for determining the typical trajectories. This analysis was extended to stratified oscillating flows [*Boyer and Zhang*, 1990a, 1990b; *Zhang and Boyer*, 1993]. Little interest seems to have been brought so far to rectification effects associated with the presence of canyons although canyons by themselves have been recognized as having possible important dynamical influences for example in the Mediterranean [*Maso et al.*, 1990].

The purpose of the present study is to explore the flow characteristics, including rectified currents, resulting from a homogeneous, zero-mean, oscillatory motion past over a submerged elongated bank next to a vertical wall boundary and over a canyon in an otherwise infinitely long shelf break of constant cross-section. The general emphasis is on obtaining a better understanding of the motion fields produced by the interaction of oscillatory background motions with idealized topography. But more specific interest is with considering how longitudinal variation of the transverse topographic gradients may be a source of rectification. Both numerical and laboratory approaches are used so that intercomparisons can lead to a deeper understanding of the physical processes involved. So far only numerical computations have been used in the canyon case but laboratory investigations are underway.

Case	Ro	Ro_t	X
1	0.041	0.40	0.32
2	0.041	0.60	0.22
3	0.041	0.80	0.16
4	0.041	1.20	0.11
5	0.081	0.60	0.43
6	0.081	0.80	0.32
7	0.081	1.20	0.21
8	0.081	1.59	0.16
9	0.122	0.60	0.64
10	0.122	0.80	0.48
11	0.122	1.20	0.32
12	0.122	1.59	0.24
13	0.127	0.16	2.50
14	0.139	0.22	2.00
15	0.134	0.28	1.50

Table 1. Dimensionless parameters for the various numerical and laboratory experiments performed over the bank.

The layout of the paper is as follows. In Section 2, the physical and numerical model systems are presented. In Section 3 the results obtained with the bank obstacle are discussed. Section 4 relates the results for the rectified flow over the canyon. Finally in Section 5, general conclusions are being presented.

Model System

Physical and model flow

In this work, we consider the interaction of an oscillating, along-shore current with (i) an elongated topographic bank located along a vertical side wall (Figure 1) and (ii) a canyon cutting an infinite length shelf break (Figure 2). The same bank model was used for both the laboratory and numerical experiments.

The bank. A layer of homogeneous fluid is confined by a rectilinear wall. The depth of this layer is H. The system rotates about a vertical axis with an angular velocity Ω (Coriolis parameter $f = 2\Omega$). A bank, whose maximum height is h_0, is placed along the wall. The horizontal direction along the coast is denoted as x, y is the direction normal to the coast, while z is vertically upward. The origin of this cartesian coordinate system is at the free surface along the coast (wall), at the center of the topographic feature. In the mid-transverse section, the height of the bank is defined as:

$$\begin{aligned} h &= h_0 & 0 < y < D/2 \\ h &= h_0 \cdot cos^2 \pi (y - D/2)/D & D/2 < y < D \\ h &= 0 & y > D \end{aligned} \quad (1)$$

But relation (1) also describes the profile for a vertical section at all locations along the perimeter of the bank. The characteristic along-shore dimension, L, is defined as the length of the flat plateau along the coast.

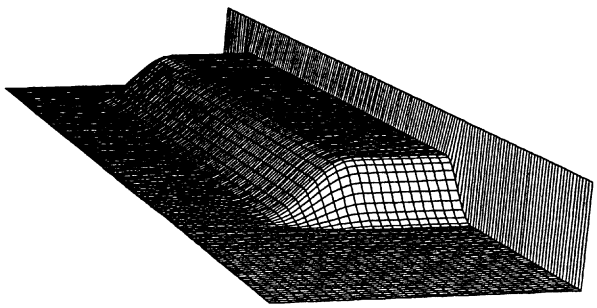

Figure 1. Perspective view of the bank. The forcing flow is parallel to the main bank direction.

The canyon. In this case, we consider a homogeneous fluid which flows over an infinite length shelf break, the height of which is given by

$$\begin{aligned} h &= h_0 & 0 < y < D \\ h &= h_0 \cdot cos^2\pi(y-D)/2D & D < y < 2D \\ h &= 0 & y > 2D \end{aligned}$$

A canyon is present in this shelf break, the horizontal shape of which is also given by a cos^2 profile.

In both situations, an oscillatory current is flowing in the direction parallel to the coast and is defined by

$$U = U_1 \cdot sin(\omega t),$$

where U_1 and ω are the amplitude (uniform in space) and the frequency of the current. The mean forcing velocity during one-half cycle of the flow oscillation

$$\overline{U}_1 = 2/\pi U_1$$

is taken to be the characteristic velocity scale. The width scale of the shelf break, D, is chosen as the characteristic lateral length scale.

It is convenient to characterize the system by the following non-dimensional parameters:

$$\begin{aligned} Ro &= \overline{U}_1/fD, \\ Ro_t &= \omega/f, \\ E_h &= A_h/fD^2, \quad E_v = A_v/fH^2, \\ Fr &= f^2D^2/gH; \end{aligned}$$

i.e. respectively the (spatial) Rossby number, the temporal Rossby number, the horizontal and vertical Ekman numbers and the Froude number. There also geometrical non-dimensional parameters such as the aspect ratios H/D, h_0/D and L/D. A_h and A_v are assumed to be constant eddy viscosity coefficients in the horizontal and vertical dimensions, respectively. In the laboratory, A_h and A_v are taken to be as the kinematic viscosity ν and g is the gravitational acceleration. Note that the Reynolds number can be expressed from the previous numbers as $Re = \overline{U}_1 D/A_h = Ro/E_h$. It is also convenient to define X as the normalized distance travelled by an undisturbed fluid parcel in one-half of a flow cycle

$$X = \pi\overline{U_1}/\omega D = \pi Ro/Ro_t$$

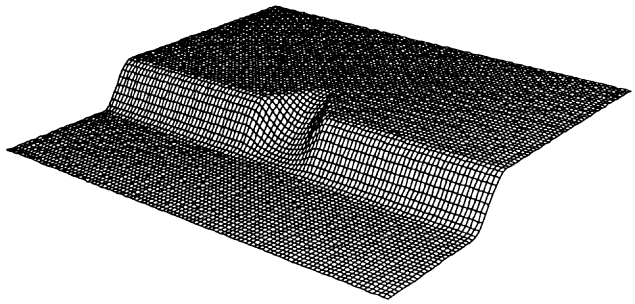

Figure 2. Perspective view of the canyon. The forcing flow is parallel to the main shelf break direction.

The laboratory experiments

The laboratory experiments were carried out on the large rotating table at the Institut de Mécanique de Grenoble. This 14 m diameter rotating platform is equipped with a 13 m diameter, 1.2 m deep cylindrical tank. For the purposes of laboratory convenience, the configurations of Figures 1 and 2 must be adapted to a circular geometry. The obstacle is placed along the wall. Its shape is defined by (1) with $D = 1$ m, $L = 5$ m and $h = 0.3$ m. The tank is filled with fresh water, the total fluid depth of which is $H = 0.35$ m. The background flow is established by oscillating the platform with an angular rotation Ω given by

$$\Omega = \Omega_0 + \Omega_1 \cdot sin(\omega t)$$

with $\Omega_0 = 0.125$ s^{-1} and $\Omega_1 \ll \Omega_0$. Such a system is dynamically equivalent to a current fluctuating over a fixed bottom.

Because $\Omega_1 \ll \Omega_0$ the Coriolis parameter f can be considered as constant and equal to $f = 0.25$ s^{-1}. The inertial period is therefore 25 s and the background rotation period $2\pi/\Omega_0$ is 50 s. Thus we are simulating an oscillatory movement parallel to a coast. The tangential velocity at $r = 6$ m is chosen as the reference velocity, $U_1 = \Omega_1 r$, and then used to define the mean forcing velocity $\overline{U_1}$. The geometrical parameters and the Ekman number are constant in the experiments. The only varied parameters are thus Ro and Ro_t.

In the laboratory, the topographic slope may be exaggerated because H/D is not a similarity parameter. The Froude number, Fr, is such that $Fr \ll 1$ support-

ing the assumption that external gravity waves do not primarily affect the situation under investigation. The Ekman numbers are small and thus viscous effects in the fluid interior, including the shelf slope region, are small away from the lateral boundaries. As discussed by *Pedlosky* [1979], a scale for the relative thickness of the vertical Ekman layer is given by

$$\delta_v/H = E_v^{1/2}$$

Regarding the effect of the side-wall, the same author proposes a scale for the lateral boundary layer thickness (Stewartson layer) as

$$\delta_h/D = E_h^{1/2}/E_v^{1/4}$$

As estimated from the above relations, the side-wall boundary layer is expected to be significantly larger than its bottom counterpart; i.e. $\delta_v \ll \delta_h$. It is clear, however, that in the vicinity of the coastline, the bottom Ekman layer will influence the nature of the flow in that region.

The velocities in the tank were measured at six locations (y = 0.25, 0.5, 0.65, 0.75, 0.85 and 1.1 m) along three radii, at $x = -1.5$, 0 and 1.5 m, at $z = -2.5$ cm below the free surface. Vertical velocity profiles were also determined for three experimental conditions. The velocities were measured by ultra-sonic current meters. In addition, we recorded the trajectories of surface floats and used image processing to obtain an overall view of the characteristic flow patterns. Dye tracers were also used to visualize the fluid movements and check the general behavior recorded by the current meters and the floats.

The numerical model

The numerical model used is the tri-dimensional primitive equation model introduced by *Haidvogel et al.* [1991] written in its channel configuration version. This model is based on the standard Navier-Stokes equations for a rotating fluid in which the hydrostatic, Boussinesq and incompressibility approximations have been made. In addition, the rigid lid approximation is assumed for filtering external gravity waves. This saves substantial amounts of computing time by permitting larger time steps. This approximation is justified by the smallness of the Froude number, Fr, as noted above. Note that while the rigid lid approximation does not allow the free surface to slope, it can nevertheless accommodate pressure gradients, thus simulating a free-surface slope, in particular cross-stream.

The model system is configured in a channel geometry where L_X and L_Y are respectively the channel length and width. Periodic boundary conditions are applied in the longitudinal direction of the channel. No-slip numerical boundary conditions are applied along the wall next to the bank. For simplicity, a slip condition is assumed on the opposite wall which, in any case, has negligible influence on the flow over the bank. Note that keeping the slip boundary condition on the opposite wall avoids grid refinement in that region and the associated increase in computational cost. In the canyon case, the slip boundary condition was implemented for both channel walls. The possible large downstream extent of the rectified flow induced by the canyon has obliged us to implement a buffer zone at the downstream part of the the channel in order to damp flow perturbations. In the buffer zone, the lateral friction is progressively increased to 10 times the actual fluid viscosity. For this same reason the channel length has also been significantly extended with regard to the bank case.

The ability of the *Haidvogel et al.* [1991] model to handle a variable grid was used to refine resolution where needed. It is indeed useful to solve for the nonlinear interactions more precisely in regions where they are expected to be more active. This is the case over the steepest shelf break gradients and along the vertical wall next to the obstacle in the bank case.

The lateral viscosity coefficient A_h was chosen as $1.3 \times 10^{-4} m^2/s$ leading to a horizontal "numerical" Ekman number of $E_h = A_h/fD^2 = 5.3 \times 10^{-4}$. This choice results from a compromise between having the finest possible grid resolution (and the related smallest possible lateral viscosity required for numerical stability) and conserving computational capabilities. The number above, while significantly larger than the typical Ekman number for the laboratory, is considered as an acceptable order of magnitude for the ocean [*Pedlosky*, 1979]. Since we assume no bottom friction and no vertical friction in the fluid interior, the vertical eddy viscosity coefficient, A_v, is zero.

The numerical model employed a channel domain with limited streamwise and crossstream extent. The channel dimensions were chosen in order that neither the opposite wall nor the channel extremities significantly influenced the flow in the regions of interest.

The parameters used, apart from viscosity, are identical to the ones in the laboratory experiments: $H = 0.35\ m$, $h_0 = 0.30\ m$ and $f = 0.25\ s^{-1}$. The length of the bank is $L = 5\ m$ and the one of the canyon $L = 1\ m$. The width of the bank is such as $D = 1\ m$ and for the canyon $D = 0.5\ m$. For the bank, we choose $L_X = 20\ m$. A width of $L_Y = 4\ m$ was found to be sufficient to ensure that the "deep ocean" side wall did not perturb the flow in the vicinity of the topographic feature. For the canyon, we choose $L_X = 15\ m$ and $L_Y = 4\ m$.

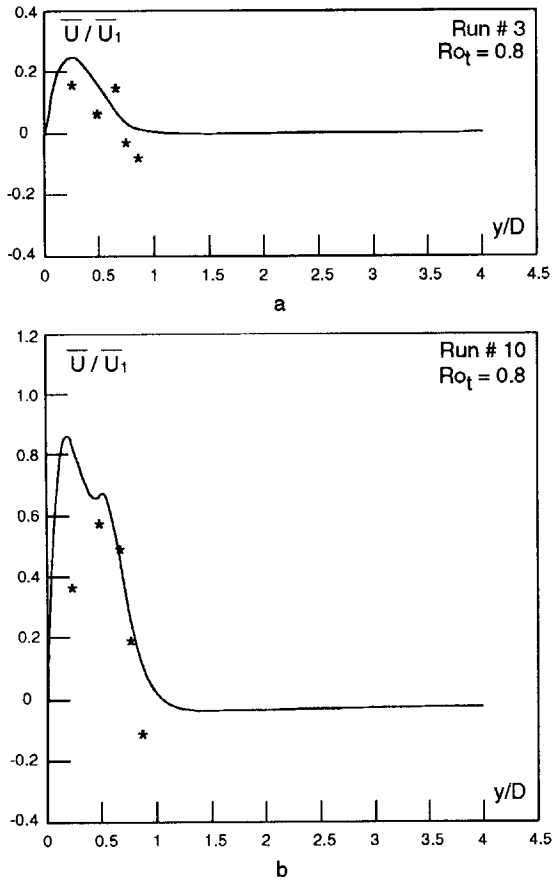

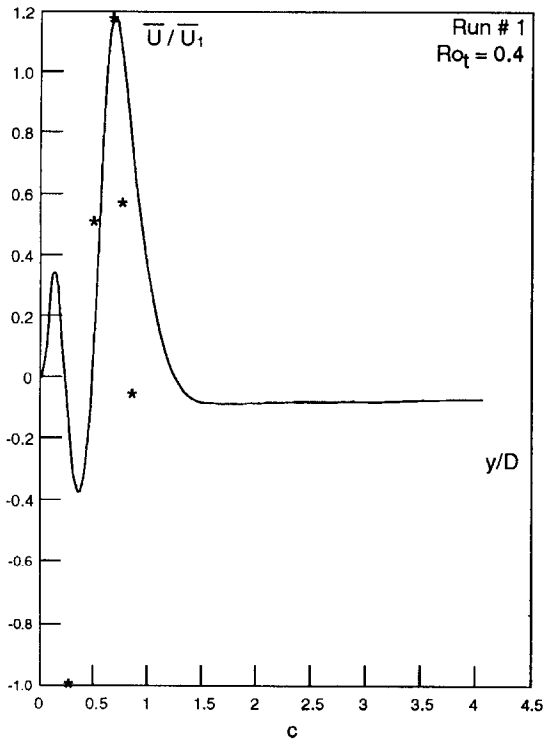

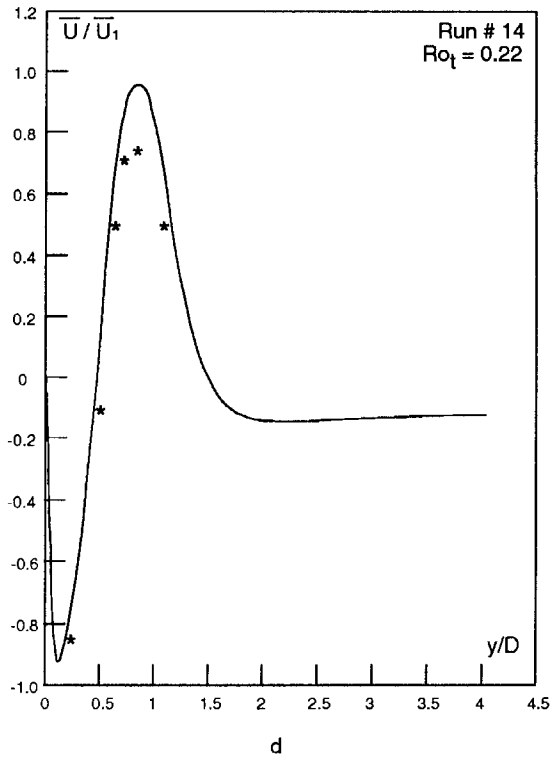

Figure 3. Typical velocity profiles $\overline{U}/\overline{U_1}$ in the mid-section. Runs # 3 (a), # 10 (b), # 1 (c) and # 14 (d). Computed values are shown by a solid line, laboratory measurements are indicated by stars.

The Bank Case

Fifteen experiments were performed, the conditions of which are indicated in Table 1.

In analyzing the results, attention was directed mainly to characterizing the flow based on the general nature of the rectified currents. Comparisons between the laboratory flows and the numerical computations were made for all the 15 experiments.

It was found convenient first to define the various characteristic flows in terms of the mid-section profiles of the streamwise rectified velocity component near the free surface. Figures 3a-d show some examples for Runs # 3, 10, 1 and 14, respectively. These plots present the computed (solid line) and measured (stars) u-components of the normalized residual current $\overline{U}/\overline{U_1}$ along the mid-section ($x = 0$), at $z = 2.5$ cm below the free surface. The scale is identical for all graphs. We note that, for the most part, there is good qualitative agreement between the numerical results and the laboratory experiments. It was observed that the dimensional rectified velocities measured in the laboratory may be very small; in Run # 3 for example, the maximum velocity is 1.6 mms^{-1}. The following typical flow regimes were defined after examining the various profiles:

- A "tips" flow regime. This flow is characterized by (i) a broad rectified flow $\overline{U}/\overline{U_1} < O(1)$ towards positive-x over the shelf and slope region (i.e. $0 < y/D < 1$) and (ii) a weak flow toward negative-x for $y/D > 1$, see Figures 3a, b.

- A "bank" flow regime. This flow is characterized by (i) a rectified current toward negative-x over the plateau, (ii) a current toward positive-x near the slope and over the near deep ocean region and (iii) a weak negative-x flow for $y/D > 1.5$, see Figure 3d.

- A transitional flow regime in which the flow is characterized along $y/D = 0$ by (i) a narrow rectified current toward positive-x along the coast, (ii) a narrow current toward negative-x on the plateau to the left of the shelf break, (iii) a strong flow toward positive-x over the slope region and (iv) a weak negative-x flow for $y/D > 1$, see Figure 3c. Along $y/D = 1.5$, the profile is the same as that along $y/D = 0$ for the bank flow regime, and along $y/D = -1.5$ it is the same as that corresponding to $y/D = 0$ for the tips flow regime.

Figures 4 a-b are typical plots of the model, horizontal, rectified velocity field for the tips and bank flow regimes, respectively. Figure 4a for the tips regime

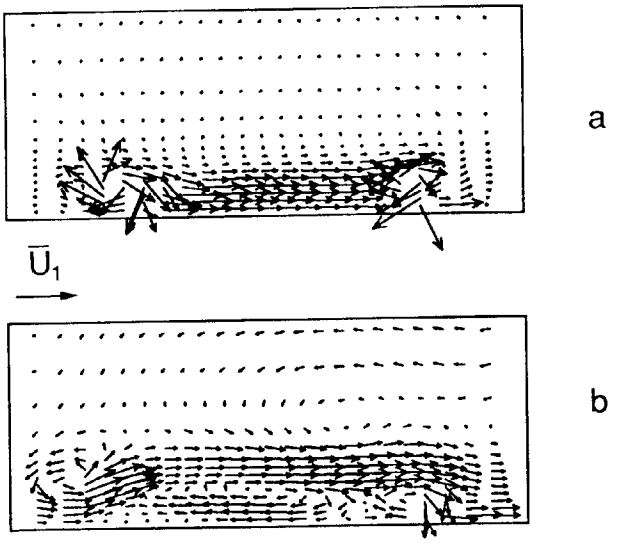

Figure 4. Examples of model horizontal velocity fields in typical tips (Run #6) and bank (Run #13) flow regimes. (The actual computational domain is larger than the ones focused on here).

(Run # 6) shows that the rectified flow for the major portion of the ridge is uni-directional towards positive-x, while strong anticyclonic eddy structures are located over the tips of the topography. In Figure 4b for the bank flow regime (Run # 13), on the other hand, the rectified flow shows a strong anticyclonic cell over the plateau and slope region, with cyclonic and anticyclonic eddy structures above the left and right tips of the topography respectively.

The vertical structure of the flow was assessed in the laboratory by measuring the time-dependent horizontal velocity as a function of depth at selected locations. The principal conclusion is that the rectified flow, within experimental error, is roughly independent of height. This also validates the model approximation of a homogeneous vertical structure.

First and foremost we found that, considering the complexity of the physical system addressed and the simplifications used in the numerical model, there is fairly good agreement between the laboratory and numerical experiments.

The study raises the consideration of the origin of the rectified current. The possible mechanisms for flow rectification are the effect of the bathymetric variation and the frictional effects. It will be recalled that bottom friction was neglected in the numerical model and thus that frictional effects enter the numerics only by lateral friction. The good agreement between the laboratory and numerical experiments suggest that bottom friction is thus proven not to be an essential ingredient of the rectification process observed in the laboratory. Moreover, scaling arguments led us to hypothesize that lateral friction is also not of leading order importance away from the wall. Bathymetric variation alone would thus appear to be the main causal factor for the observed rectified currents. Thus, in a similar way as in *Boyer et al.* [1991], the production of relative vorticity induced by bathymetric change may account for most of the rectified current.

It is of particular interest to look at the maximum values of the rectified current in the different cases with respect to the non-dimensional controlling parameters. Figure 5a shows a plot of the normalized maximum rectified current in the positive-x direction $\overline{U}_{\max}/\overline{U_1}$ as a function of Ro_t^{-1} for both the laboratory and the numerical experiments. Again good agreement is seen between the laboratory and the numerical results, although the latter are often larger. The data in Figure 5a from this limited experimental program strongly suggest that the principal parameter determining the qualitative nature of the resulting flow fields is the temporal Rossby number, Ro_t. Some of the data scatter is due to the fact that the observable $\overline{U}_{\max}/\overline{U_1}$ is also a function of Ro. Interestingly, it appears that the quantity $\overline{U}_{\max}/\overline{U_1}$ is maximum when $Ro_t^{-1} \approx 1.7$, i.e. when the forcing period is approximately twice the inertial period.

Figure 5b presents the same quantity $\overline{U}_{\max}/\overline{U_1}$ as a function of X, the normalized flow excursion during one half of the oscillatory cycle. The data collapse is similar to that of Figure 5a. Because $X \sim Ro/Ro_t$ this reinforces the fact that Ro is playing a limited role and provides additional support for the idea that the

principal governing parameter is Ro_t^{-1}. Figure 5b also reveals that the rectified velocity maximum occurs for $X \approx 0.5$, i.e., when the flow excursion approximates the width of the slope region.

Two different types of behavior can further be identified on Figures 5a and 5b: (i) a range for which the rectified velocity increases approximately linearly with Ro_t^{-1} and X ($0 < Ro_t^{-1} < 2$; $0 < X < 0.5$) and (ii) a range in which the velocity decreases with Ro_t^{-1} and X ($Ro_t^{-1} > 2$; $X > 0.5$). Within the range of parameters being investigated, the maximum velocity reached in the mid-section is about 1.5 $\overline{U_1}$, which is approximately equal to $\pi/2 \cdot \overline{U_1} = U_1$. No rectified flows exceeding U_1 were found in any of the experiments at any location. The maximum amplitude of the rectified flow seems therefore constrained in all cases by $\overline{U} < U_1$, i.e., by the maximum amplitude of the incident forcing flow. Note that this maximum value is reached approximately at the transition point between the tips and bank flow regimes.

Using all these results it was possible to classify the experiments of Table 1 according to the previous general definitions and to draw a flow regime diagram in (Ro_t, Ro) parameter space (Figure 6). The respective run numbers are also indicated with reference to Table 1. This diagram clearly shows the dominance of Ro_t in determining flow regimes.

Figure 7 summarizes the way in which maximum normalized rectified velocity $\overline{U}_{\max}/\overline{U_1}$ in the mid-section $x = 0$, varies in (Ro, Ro_t) parameter space. As in Figure 5a, it shows that the rectified flow amplitude has a maximum for $Ro_t \approx 0.5$, i.e., when the forcing flow oscillation is twice the inertial period.

A number of remarks may usefully be made about the so-called tips and bank flow regimes. As stated earlier, for the largest values of Ro_t, we observe the tips flow regime in which the rectified flow in the mid-bank portion is very weak. This is consistent with previous studies showing that rectification does not occur in the along-shore direction for an along-shore oscillatory current along a coastline of uniform cross-section. In the absence of other mechanisms, such as non-linear bottom friction, an infinite length obstacle like this will not give rise to any rectification [*Haidvogel and Brink*, 1986]. This result was checked numerically in the present case by extending the obstacle length L to infinity. This can also be seen simply as a consequence of simple analytical considerations (see e.g. *Verron et al.*, 1994), which suggest no rectification from an oscillatory flow parallel to the bank slope.

The basic rectification processes over the bank could therefore be interpreted as follows. The longitudinal variations of the transverse bathymetric gradients where they exist (tips) initiate local rectification ($U.\nabla H \neq 0$) and, where they are absent (mid-bank slope) local rectification is also lacking ($U.\nabla H = 0$). Thus, when the flow excursion is at the scale of the tips ($X \sim D$),

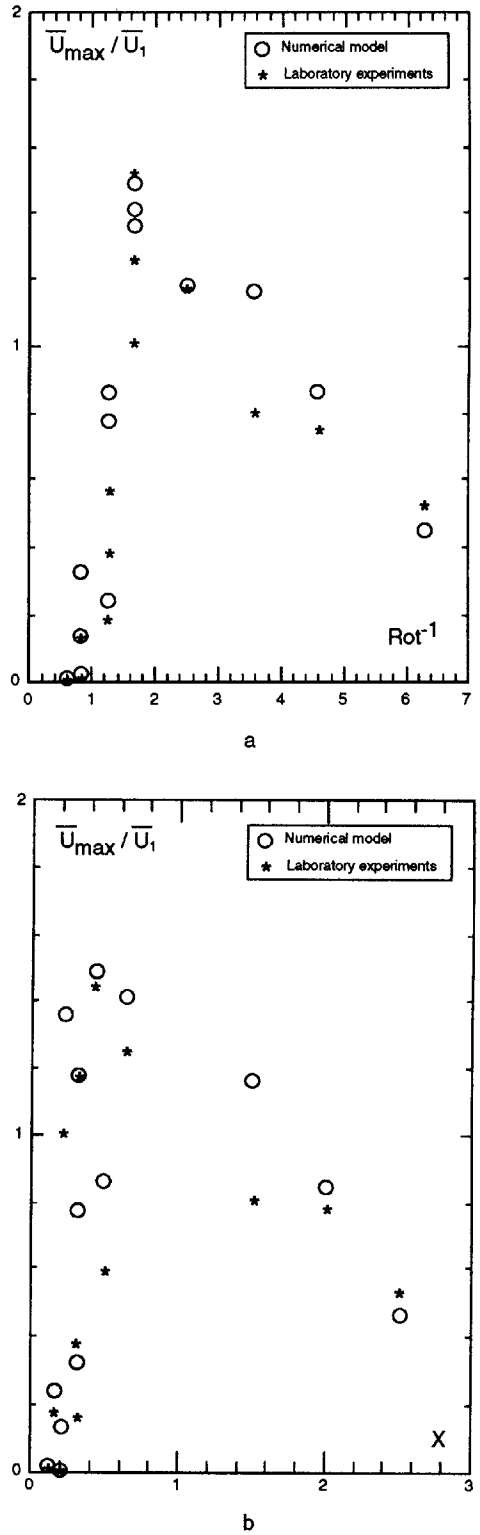

Figure 5. Maximum rectified velocity in the mid-section as a function of Ro_t^{-1} (a) and X (b).

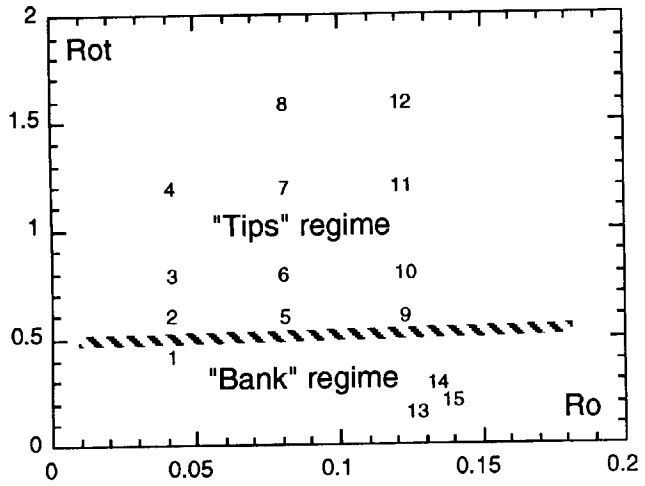

Figure 6. Flow regime diagram in the (Ro, Ro_t) parameter space.

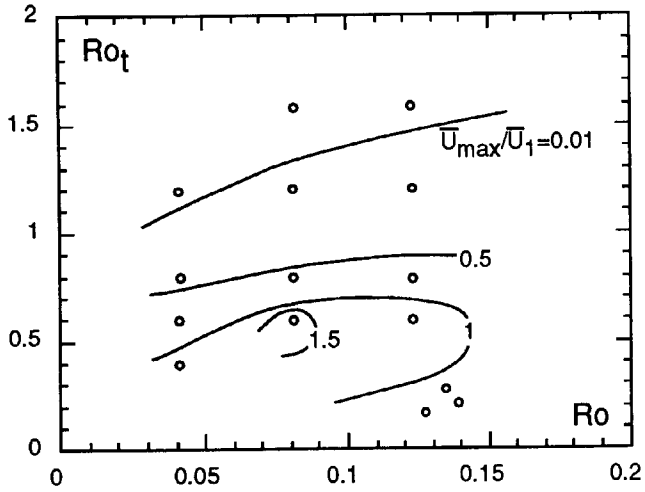

Figure 7. Maximum rectified velocity in the mid-section in the (Ro, Ro_t) parameter space.

rectification stays confined to the tips and remains weak at mid-bank. For such cases, the tips flow regime is observed. When the flow excursion is at the scale of the characteristic streamwise length of the bank ($X \sim L$), the rectifying effects of the tips are sufficient for the whole bank to be taken over. The bank flow regime is then observed. In a word, one could say that longshore rectified currents are present only because the bank has tips.

This study indicates the importance of along-shore variations in the shelf break geometry. It suggests that off-shore canyons and ridges will strongly affect the rectification patterns resulting from along-shore oscillatory currents and motivates the second part of this investigation over a simplified canyon feature.

The Canyon Case

We have investigated 16 situations corresponding to the sets of controlling parameters indicated in Table 2.

Figures 8a and 8b show typical situations observed in the study. For each figure, the mean streamfunction and vorticity patterns are shown as well as the mean velocity vectors pattern. A general description of the flow pattern can be made looking at the velocity vectors and is globally valid for all cases: a rectified flow is generated along the longitudinal direction of the shelf break. This

Case	Ro	Ro_t	X
1	0.05	0.25	0.628
2	0.10	0.25	1.257
3	0.15	0.25	1.885
4	0.20	0.25	2.513
5	0.05	0.50	0.314
6	0.10	0.50	0.628
7	0.15	0.50	0.942
8	0.20	0.50	1.257
9	0.05	0.75	0.209
10	0.10	0.75	0.419
11	0.15	0.75	0.628
12	0.20	0.75	0.838
13	0.05	1.00	0.157
14	0.10	1.00	0.314
15	0.15	1.00	0.471
16	0.20	1.00	0.628

Table 2. Dimensionless parameters for the various numerical experiments over the canyon.

rectified flow has a mean direction meandering over the canyon area, first towards the abysses, then towards the shelf, then back to the abysses, to finally stay more or less rectilinear, parallel to the shelf break and mostly confined at the upper part of the break. The current meandering over the canyon is more or less in spatial phase with the canyon structure. The intensity of the rectified flow is strongly dependent on the flow parameters. The mean flow meandering pattern corresponds to a succession of alternating eddies, positive, negative and positive, over the canyon region. The intensities of these eddies and their precise positions with regard to the canyon are a function of the flow parameters.

The most noticeable dynamical feature in many situations is the existence of a downstream mean current along the shelf break which can radiate in some cases far from the canyon area. Figure 9 presents one example of the section of the rectified current velocity one meter downstream the middle of the canyon. The velocity profile in all cases is very much centered at the top part of the shelf break, i.e. at the location where the topographic height is decreasing. This profile is rather sharp. An horizontal width scale based on the e-folding factor would be something like the canyon scale D. It

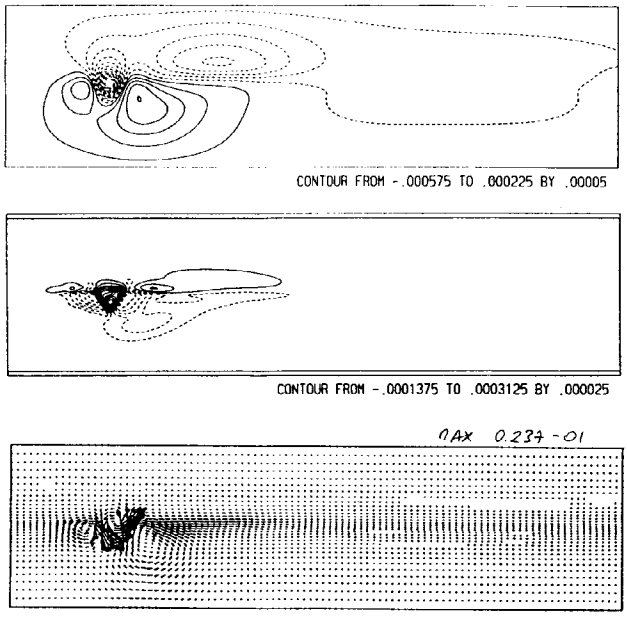

(a)

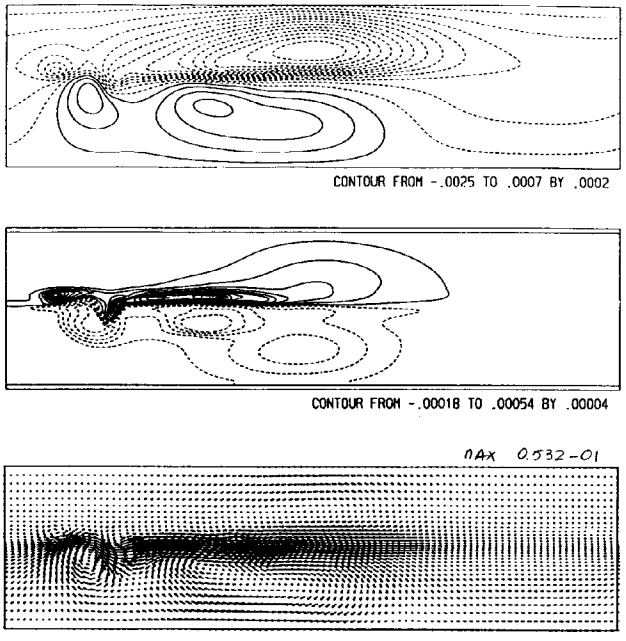

(b)

Figure 8. Examples of mean rectified streamfunction, vorticity and velocity fields over the canyon for Run # 16 (a) and Run # 3 (b).

is also noted that a small transverse asymmetry in the velocity profile is observed with the increase of Ro_t.

It is possible in particular to analyse the variation of the rectified current maximum velocity induced over the canyon (sections performed right in the middle of the canyon) and one meter downstream. The results are shown in Figures 10a and 10b, respectively, as a function of Ro_t^{-1}. The data scatter with regard to Ro_t

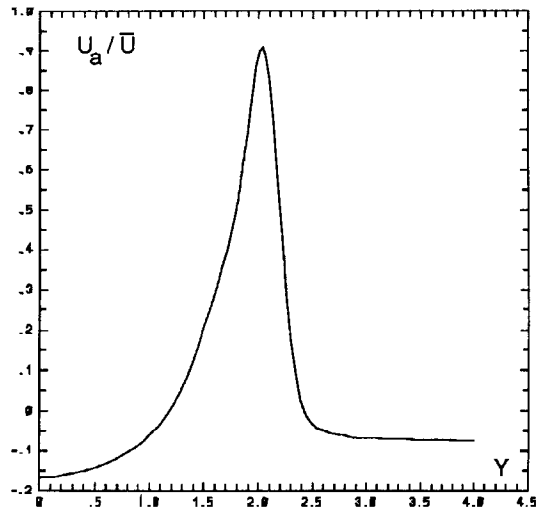

Figure 9. Example of mean rectified velocity transversal profile at a distance of one m downstream of the middle of the canyon for Run # 3.

is relatively large which would show that Ro_t is not as clearly the leading parameter for the rectified flow amplitude as in the bank problem. Things must however be said cautiously. Indeed, data scatter is most important in the case of the mid-canyon rectified flow rather than in the case of the downstream rectified flow. The mean flow pattern within the canyon is rather complex and the averaging procedure may have residuals due to insufficient convergence. Conversely, the flow pattern downstream has a more stable configuration and may be of greater interest. The downstream maximum flow amplitude is more satisfactorily described in terms of the parameter Ro_t although some noticeable impact of Ro is visible.

With regard to the control parameter R_0, Figure 11 shows that the velocity maximum amplitude for the downstream flow reveals two main things: (i) there are clearly two main regimes of rectified flow intensities, a "slow" downstream rectified flow for the largest values of Ro_t ($Ro_t = 0.75$ and 1.00) and a "fast" downstream rectified flow for the smallest values of Ro_t ($Ro_t = 0.25$ and 0.50), (ii) for the "slow" regimes, the velocity amplitude increases with Ro while, for the "fast" regimes, the velocity amplitude roughly decreases with Ro. Note that, similar to the bank case, the rectified flow intensity can be as large as the forcing. By looking at all of the data obtained, it is tempting to say that, similar to the bank problem, there are two rectified flow regimes over the canyon:

- a "local" regime in which the rectified flow is roughly confined to the canyon area without really affecting neighbouring regions (analogous to the "tips" regime),

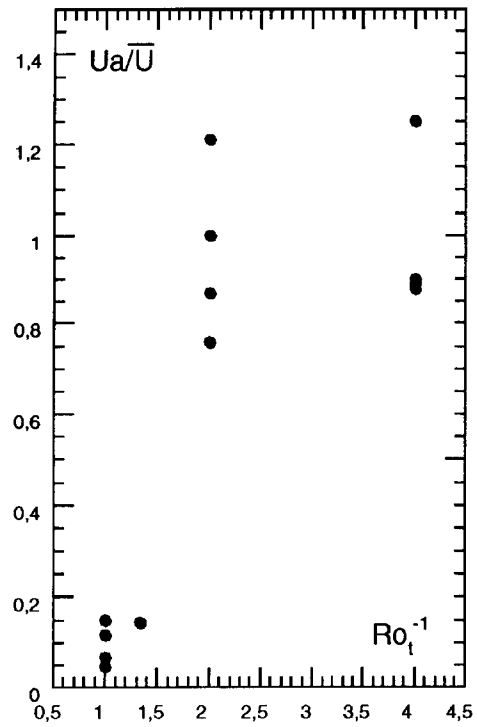

Figure 10. Maximum rectified velocity as a function of the temporal Rossby number Ro_t at a distance of oneone m downstream of the middle of the canyon (a) and at mid-canyon (b).

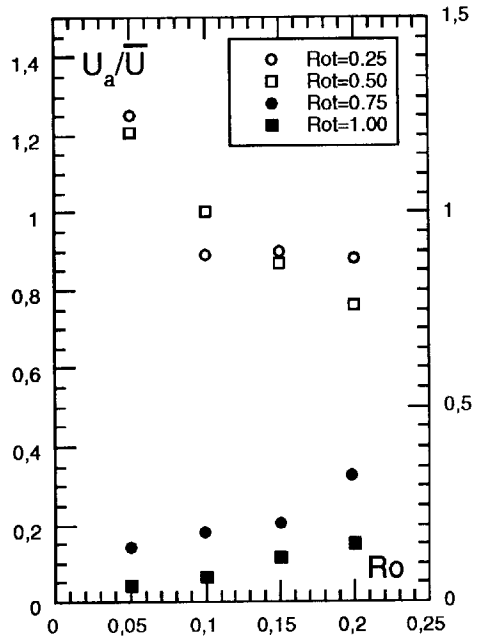

Figure 11. Maximum rectified velocity as a function of the Rossby number R_0 at a distance of one one m downstream of the middle of the canyon.

- a "non-local" regime in which the rectified flow due to the canyon extends away from the originating area (analogous to the "bank" regime).

This non-local regime is clearly of much interest since it would indicate that a canyon of limited geographical extent may have influence at large distances. Figure 12 focusses more information on this point by plotting the approximate length of penetration of the rectified flow pattern (non-dimensionalized by D) in the controlling parameter space. This penetration length, L_P, is measured from the middle axis of the canyon and is estimated approximately from the mean streamfunction/vorticity pictures for all cases. The larger Ro_t (and smaller Ro) correspond to the smallest values of L_P/D, i.e. to the "local" regime. One must be cautious when considering the largest L_P/D since the "buffer zone" employed in the model for treating the open boundary condition problem as already mentioned, may spuriously damp the downstream penetration at large distances.

Conclusions

Firstly, the interaction between an along-shore oscillatory current and an elongated bank placed along a vertical wall was investigated by means of laboratory and numerical experiments. The main conclusions focus on the intense rectified currents which are observed

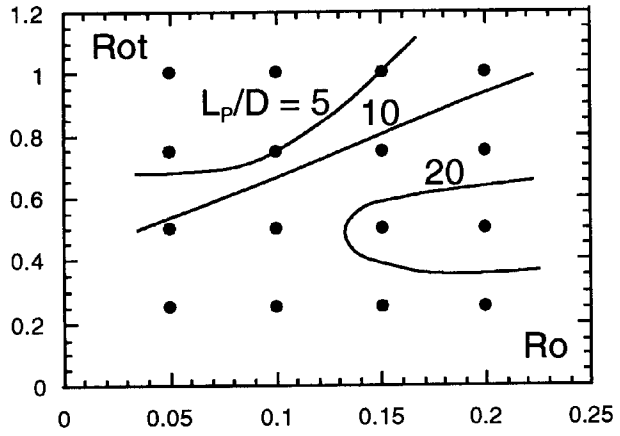

Figure 12. Approximate length of penetration for the rectified mean current over the canyon in the (Ro, Ro_t) parameter space.

over the bank and along the coast. These rectified currents are mainly controlled by the topographic influences of the tips; i.e. by the most significant longitudinal variations of the transverse topographic gradients. The study has demonstrated the crucial role of the temporal Rossby number in determining the general nature of the characteristic flow patterns. For large Ro_t, one observes the tips regime in which the rectified flow over the mid-bank is unidirectional, but relatively weak. For small Ro_t, one obtains a relatively strong anticyclonic rectified flow pattern over the entire topographic feature, i.e., the flow near the mid-bank has the coastline on the right over the shelf break, but reverses in direction near the coast.

Secondly, the interactions between an along-shore oscillatory current and a canyon in an otherwise long shelf break of constant cross section was investigated by numerical simulations. The main conclusion focuses on the possible large, downstream (i.e. with the shallow fluid on the right), range of action that the canyon may have in terms of rectification. The horizontal scale associated with the rectified mean current penetration may for example be typically of one order of magnitude larger than the horizontal scale of the canyon itself. This may have important physical consequences as it shows that through the process of rectification, a simple canyon topographical irregularity may have large distance effects. Two flow regimes were observed which have strong similarities with the "tips" and "bank" regimes. The controlling parameter is mainly Ro_t as it was also in the case of the bank. But the influence of Ro is, however, more clearly sensitive here. As in the bank case, the intensity of the rectified current may be of the order of the amplitude of the forcing current. A tidal forcing velocity may for example generate a mean rectified current of the same velocity amplitude.

The complex role of bottom boundary layers has not been investigated (and lateral boundary for the bank situation) and is therefore not well-understood at this time. The good agreement between the laboratory experiments and the numerical model in the first part of the present study, however, suggests that the present model is dominated by topographic effects and thus captures most of the physics involved in the rectification process. The present study has also neglected stratification effects which should be considered to be important in most oceanic applications. Although the present models are crude representations of real flows, it is suggested that the basic mechanisms leading to flow rectification are representative of physical mechanisms at work in nature.

Acknowledgments. This work was supported by the Centre National de la Recherche Scientifique (CNRS-INSU). The calculations were made possible by the numerical facilities of the Centre de Calcul Vectoriel pour la Recherche in Palaiseau. The support of the Ocean Sciences Division of the U.S. National Science Fundation is also acknowleged.

References

Boyer, D.L. and Zhang, X., 1990a: The interaction of time-dependent rotating and stratified flow with isolated topography, *Dyn. Atmos. Oceans*, 14, 543-575.

Boyer, D.L. and Zhang, X., 1990b: Motion of oscillatory currents past isolated topography *J. Phys. Oceanog.*, 20, 1425-1448.

Boyer D.L., G. Chabert d'Hières, H. Didelle, J. Verron, R.R. Chen and L. Tao, 1991: Laboratory simulations of tidal rectification over seamounts: homogeneous model. *J. Phys. Oceanogr.*, (21) 10, 15559-1579.

Brylinski, J.M. and Lagadeuc, YL, 1990, The inshore/offshore waters interface off the French coast in Dover Strait: a frontal area, *C.R. Acad. Sci. Paris*, t. 311, Serie II, 535-540

Butman B., R.C. Beardsley, B. Magnell, D. Frye, J.A. Vermesch, R. Schlitz, R. Limeburner, W.R. Wright and M.A. Noble, 1982: Recent observations of the mean circulation on Georges bank. *J. Phys. Oceanogr.*, 12, 569-591.

Chen, C., 1992, Variability of current in Great South Channel and over Georges Bank: observations and modelling, Ph.D. Dissertation, Massachusetts Institute of Technology and Woods Hole Oceanographic Institution, 283 pages

Ericksen, C. 1991, Observations of amplified flows atop a large seamount, *J. Geophys. Res.*, 96 (C8), 15.227-15.236

Garreau P. and R. Mazé, 1992: Tidal rectification and mass transport over a shelf break: a barotropic frictionless model. *J. Phys. Oceanogr.*, 22 (7), 719-731.

Genin, A., Noble, M. and Lonsdale, P.F., 1989, Tidal currents and anticyclonic motions on two North Pacific seamounts, *Deep-Sea Res.*, 36, 1803-1816

Haidvogel D. B. and K. H. Brink, 1986: Mean currents driven by topographic drag over the continental shelf and slope., *J. Phys. Oceanogr.*, 16, 2159-2171.

Haidvogel D. B., J. Wilkin and R. Young, 1991. A semi-spectral primitive equation ocean circulation model using vertical sigma and orthogonal curvilinear horizontal coordinates. *J. Comp. Phys.*, 94, 151-185.

Holloway G., 1987: Systematic forcing of large scale geophysical flows by eddy-topography interaction. *J. Fluid Mechanics*, 184, 463-476.

Huthnance, J.M., 1973, Tidal current asymmetries over the Norfolk Sandbanks, *Estuarine and Coastal Marine Science*, 1, 89-99

Huthnance, J.M., 1981, On mass transports generated by tides and long waves, *J. Fluid Mech.*, 102, 367-387

Loder, J.W., 1980, Topographic rectification of tidal currents on the sides of Georges Bank, *J. Phys. Ocean.*, 10, 1399-1416

Loder, J.W. and Wright, D.G., 1985, Tidal rectification and frontal circulation on the sides od Georges Bank, *J. Mar. Res.*, 43, 581-604

Maas, L.R.M. and van Haren, J.J.M., 1987, Observations on the vertical structures of tidal and inertial currents in the North Sea, *J. Mar. Res.*, 45, 293-318

Maas, L.R.M. and Zimmerman, J.T.F., 1989a, Tide-topography interactions in a stratified shelf sea: I- Basic equations for quasi-nonlinear internal tides, *Geophys. Astrophys. Fluid Dyn.*, 45, 1-35

Maas, L.R.M. and Zimmerman, J.T.F., 1989b, Tide-topography interactions in a stratified shelf sea: II- Bottom trapped internal tides and baroclinic residual currents, *Geophys. Astrophys. Fluid Dyn.*, 45, 37-69

Maso M., P. E. La Violette and J. Tintore, 1990: Coastal flows modificiation by submarine canyons along the NE Spanish coast. *Sci. Mar.*, 54 (4), 343-348.

Pedlosky J., 1979: Geophysical fluid dynamics. Springer-Verlag. New York Heidelberg Berlin.

Pingree, R.D. and Le Cann, B., 1990, Structure, strength and seasonality of the slope currents in the vicinity of the Bay of Biscay region, *J. Mar. Biol. Ass. U. K.*, 70, 857-885

Robinson I.S., 1981: Tidal vorticity and residual circulation. *Deep Sea Research*, 28 A, 3, 195-212.

Stommel, H., 1954, Serial observations of drift currents in the Central North Atlantic Ocean, *Tellus*, 6, 204-214

Tang, Y. and K.T. Tee, 1987, Effects of mean current interaction on the tidally induced residual current, *J. Phys. Oceanog.*, 17, 215-230

Tee, K.T., 1985, Depth-dependent studies of tidally induced residual currents on the sides of Georges Bank, *J. Phys. Oceanog.*, 15, 1818-1846

Verron J., D. Renouard, D. L. Boyer, G. Chabert d'Hières, T. Nguyen and H. Didelle, 1995: Rectified flows over an elongated topographic feature along a vertical wall. To appear in the *J. Phys. Oceanog.*

Wright, D.G. and Loder, J.W., 1985, A depth dependent study of the topographic rectification of tidal currents, *Geophys. Astrophys. Fluid Dyn.*, 31, 169- 220

Zhang, X. and Boyer, D.L., 1993, Laboratory study of rotating, stratified, oscillatory flow over a seamount, *J. Phys. Oceanog.*, 23, 1122-1141

Zimmerman J.T.F., 1978: Topographic generation of residual circulation by oscillatory (tidal) currents. *Geophys. Astrophys. Fluid Dynamics*, 11, 35-47.

Zimmerman, J.T.F., 1980, Vorticity transfer by tidal currents over an irregular topography, *J. Mar. Res.*, 38, 601-630